NASA TECHNICAL NOTE

NASA TN D-4758

ANOMALOUS DIFFUSION IN A PLASMA FORMED FROM THE EXHAUST BEAM OF AN ELECTRON-BOMBARDMENT ION THRUSTER

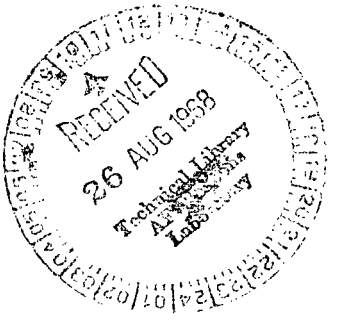

by Allan J. Cohen

Lewis Research Center
Cleveland, Ohio

NATIONAL AERONAUTICS AND SPACE ADMINISTRATION • WASHINGTON, D. C. • AUGUST 1968

NASA TN D-4758

ANOMALOUS DIFFUSION IN A PLASMA FORMED FROM THE EXHAUST BEAM OF AN ELECTRON-BOMBARDMENT ION THRUSTER

By Allan J. Cohen

Lewis Research Center
Cleveland, Ohio

NATIONAL AERONAUTICS AND SPACE ADMINISTRATION

For sale by the Clearinghouse for Federal Scientific and Technical Information
Springfield, Virginia 22151 – CFSTI price $3.00

ABSTRACT

A 10-cm-diam. cylindrical anode with a grounded coaxial center rod was immersed in the low density ($n_e \sim 2\times10^7$ cm^{-3}) exhaust beam of an ion thruster. A longitudinal magnetic field was applied. A theoretical and experimental study was made of the electron diffusion process in the beam plasma passing through the electrically floating anode. Anomalous diffusion and low frequency noise were found. The mechanism of anomalous diffusion was considered similar to that reported by Kadomtsev and Nedospasov. Bohm's diffusion equation was found applicable and a constant of 1/8 (twice Bohm's value) was deduced experimentally. Rotation in the plasma was found by means of a correlation technique. The measured frequency of rotation ranged from 100 to 150 kHz.

ANOMALOUS DIFFUSION IN A PLASMA FORMED FROM THE EXHAUST BEAM OF AN ELECTRON-BOMBARDMENT ION THRUSTER

by Allan J. Cohen

Lewis Research Center

SUMMARY

A 10-centimeter-diameter, cylindrical anode with a grounded coaxial center rod was immersed in the low density ($n_e \sim 2\times10^7$ cm^{-3}) exhaust beam of an ion thruster. A longitudinal magnetic field ranging up to 110×10^{-4} tesla was applied. A theoretical and experimental study was made of the electron diffusion process in the beam plasma passing through the electrically floating anode. Anomalous diffusion in the radial direction and low frequency noise were found. The mechanism of anomalous diffusion was considered similar to that reported by Kadomtsev and Nedospasov. Bohm's diffusion equation was found applicable and a constant (twice Bohm's value) was deduced experimentally. Rotation in the plasma was found by means of a correlation technique. The measured frequency of rotation ranging from 100 to 150 kilohertz was predictable from theory.

INTRODUCTION

A weak magnetic field is used in the discharge chamber of the electron-bombardment ion thruster (ref. 1) to lower the value of energy required to produce a beam ion and correspondingly increase efficiency. The magnetic field reduces the radial transport rate of the electrons across the discharge chamber of the ion thruster and as a result enhances performance. It has been observed that the electron diffusion process in the ion thruster falls into two regions, stable and unstable (refs. 2 and 3), and that the corresponding diffusion coefficient behaves classically and nonclassically, respectively. It also has been observed that the performance of the ion thruster is significantly enhanced by the magnetic field only when the thruster is operating in the stable region (ref. 2). According to reference 3 a critical value of the magnetic field separating stable and unstable regions can be calculated (following the Kadomtsev and Nedospasov treatment, ref. 4) for the discharge plasma of the ion thruster. It is important to note that the dis-

charge plasma not only is subjected to an axial magnetic field in the cylindrical ion-chamber configuration but also contains an applied radial electric field and a longitudinal electric field which develops from potential penetration from end wall plasma sheaths.

One of the first successful plasma diffusion theories for determining the boundary between stable and unstable, or anomalous regions of a plasma, was the Kadomtsev and Nedospasov theory (ref. 4). In this theory rotating perturbations of number density and potential are introduced in a Fourier expansion and values for the critical magnetic field and rotational frequency are obtained. The theory was applied to the high pressure ($\sim$ 1 mm) positive column in a longitudinal magnetic field. An applied axial electric field was also present. Guest, Simon, and Hoh (refs. 5 and 6) further expanded the theory to less dense plasmas and to plasmas with properties other than those of the positive column. Hoh's physical explanation of this type of anomalous diffusion (the Kadomtsev and Nedospasov type) was to suggest that a density concentration of electrons revolves in the plasma moving through the neutral background and that an ion concentration follows closely behind, but slightly separated, thus giving rise to a rotating azimuthal potential gradient. As a result a Hall drift exists, when the magnetic field strength is greater than the critical value, enhancing motion across the magnetic field and causing an enhanced loss from the "classical" containment characteristic of the magnetic field. Since then several investigations of the diffusion process in a magnetized plasma have revealed rotation (see, for example, ref. 7) and many investigations have shown increased or anomalous diffusion coefficients (ref. 8). It is the belief of some investigators (ref. 8) that any partially ionized plasma submerged in a magnetic field and having an electric field either applied or developed is susceptible to anomalous diffusion beyond some critical magnetic field or beyond a critical value of a related parameter.

Classically, the collisional diffusion coefficient in a magnetic field should behave as B^{-2} (ref. 9). Early in plasma physics experimentation, Bohm (ref. 10) made a measurement of the diffusion coefficient in a magnetic field and found that the measured value differed significantly from the classical value. He proposed a new empirical relation for the diffusion coefficient which contained a B^{-1} variation with magnetic field. He believed this to be the proper variation of the diffusion coefficient for a plasma undergoing anomalous or, as he termed it, drain diffusion. Since that time numerous experiments (ref. 8) and theories (refs. 11 to 13) have been put forward to clarify the diffusion process in a magnetized plasma.

Because of the inherent difficulties in plasma physics experiments aimed at determining transport rates, the proper value of the diffusion coefficient in a magnetized plasma is not clear, nor is the physical explanation of its unstable behavior. It is the author's belief that anomalous diffusion in a magnetized, partially ionized plasma with electric fields can be understood in terms of the mechanism used by Kadomtsev and Nedospasov to predict stable and unstable regimes of particle transport. Throughout this

report, reference to the Kadomtsev and Nedospasov theory should be taken in the broad sense to include all those theories of anomalous diffusion in partially ionized gases in which there are rotational number density and potential perturbations and in which the pertinent mechanism of transport of the perturbations is the Hall effect. This mechanism can produce the Bohm diffusion that appears to predominate in the unstable mode of the magnetized plasma (see refs. 13 to 16).

In the present report the electron diffusion process in a magnetic field is studied by floating a metal anode in the exhaust beam of an ion thruster. This configuration is studied instead of the discharge chamber process of the ion thruster because of its relative simplicity. Although an exact correspondence is not expected, certain inferences are drawn with respect to the diffusion process of the ion thruster (and also the diffusion process in general) based on similarities. Because the metal anode is floated, a radial electric field develops and electrons drift radially in the combination electric and magnetic field.

The plasma is probed for electric potential and number density gradients to determine whether the diffusion process is classical or anomalous in the range of magnetic field strengths studied. The Kadomtsev and Nedospasov theory is compared to the results obtained. The plasma is also investigated for various values of electron current flow to the anode as well as electric field strength. Bohm's equation for the mobility coefficient with its characteristic B^{-1} magnetic field dependence is then compared with these data. Finally, the plasma is studied for rotation in the unstable region by a correlation technique. As a result of this work and previous studies by other authors, conclusions are drawn about the diffusion process in a magnetic field and about the behavior of the ion thruster.

THEORY

Electron Diffusion Process

Sketch (a) shows the experimental arrangement; a schematic is given in figure 1(a). A cylindrical coordinate system with orientation as shown in sketch (a) is used throughout

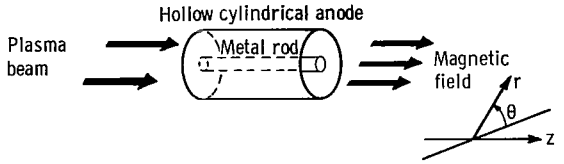

(a)

the report. An electrically floating cylindrical anode and coaxial grounded rod are set in the exhaust beam of an ion thruster. A uniform axial magnetic field is applied. The ion beam is neutralized by secondary electrons from the tank walls and other grounded equipment, forming an approximately neutral plasma for the experiment. The ion number density of the plasma n at any point can be obtained from the relation

$$J_B = neU_{zi} \tag{1}$$

where J_B is the beam current density measured in this study by a molybdenum probe and U_{zi} is the exhaust velocity (a constant) of the ion thruster. (Symbols are defined in the appendix.) The plasma beam not only has an axial velocity but also has a radial velocity component, that is, it spreads after leaving the ion thruster. As a result the anode is struck by the ion beam and, since it is electrically floating, it builds up a positive potential with respect to the grounded rod. The electrons in the plasma are pulled to the anode by this electric field and effectively neutralize it. The axial magnetic field impedes the electron flow to the anode.

The radial current density of electrons in the experiment can be deduced from the equation

$$J_{re} = -D_{\perp e}\frac{\partial n_e}{\partial r} + n_e\mu_{\perp e}\frac{\partial V}{\partial r} \tag{2}$$

where the first term is the current due to a number density gradient and the second term is the current due to a potential gradient. This equation with classical values of $D_{\perp e}$ and $\mu_{\perp e}$ is used to determine if the radial electron transport rate is classical or anomalous. The equation, with θ-dependent terms, is given in reference 5. If the radial number density gradient is neglected (experimental justification will be discussed later), the equation for electron current density across the system reduces to the following Ohm's law expression:

$$J_{re} = n_e\mu_{\perp e}\frac{\partial V}{\partial r} \tag{3}$$

From Einstein's relation (ref. 8), the result is

$$D_{\perp e} = \mu_{\perp e}\frac{kT_e}{e} \tag{4}$$

where $D_{\perp e}$ and $\mu_{\perp e}$ are the electron diffusion and mobility coefficients, respectively,

and kT_e/e is the electron temperature in electron volts. Equation (4) shows that the mobility and diffusion coefficient are directly proportional for a constant electron temperature.

Classically, from reference 5, the electron mobility coefficient (for sufficiently large values of $\omega_e\tau_e$) is

$$\mu_{\perp e} = \frac{1}{B\omega_e\tau_e} = \frac{1}{B^2}\left(\frac{m_e}{e\tau_e}\right) \tag{5}$$

where $\omega_e = eB/m_e$, $\tau_e = 1/N_o\langle\sigma v\rangle$, N_o is the neutral density (assumed to be much greater than the plasma number density n), and $\langle\sigma v\rangle$ is the velocity times the collision cross section averaged over the electron velocity distribution. Values of $\omega_e\tau_e$ for the experiment are given in table I which also lists other important experimental constants.

Bohm, however, has suggested (ref. 10) that, for anomalous or drain diffusion, the diffusion coefficient is

$$D_{\perp e} = \frac{kT_e}{e}\frac{C_B}{B} \tag{6}$$

where B is the magnetic field and the constant C_B according to Bohm is 1/16. Comparing equation (4) with equation (6) results in the corresponding (Bohm) mobility

$$\mu_{\perp e} = \frac{C_B}{B} \tag{7}$$

Equation (5) can be compared with equation (7) to show the difference between the classical electron mobility and the Bohm mobility.

In the anomalous diffusion regime, according to the Kadomtsev and Nedospasov diffusion theory, number density concentrations drift across magnetic field lines as a result of the Hall effect. In reference 13 a derivation of Bohm's equation is presented based on this (Hall) effect. In this derivation it was necessary to assume that the derived expression for the Bohm coefficient was independent of magnetic field. Reference 7 added experimental support to the derivation of reference 13.

In the present report, equation (3) is used empirically in the anomalous region to obtain a mobility coefficient that is equated to the Bohm mobility (eq. (7)) to arrive at a value for the Bohm constant C_B.

Number Density and Potential Gradient Behavior

The longitudinal and radial behavior of the number density and potential to be expected in the present experiment can be deduced from the continuity equation, the electron equation of motion, and appropriate assumptions. The continuity equation for the ions in steady state is, in vector notation,

$$\nabla \cdot (n_i \vec{U}_i) = 0 \tag{8}$$

and for the electrons is

$$\nabla \cdot (n_e \vec{U}_e) = 0 \tag{9}$$

where $\vec{U} = (1/n)\vec{J}$ and U refers to the drift velocity. Equation (3) is the equation of motion for the electrons. For application to the present experiment, the following simplifying assumptions are considered appropriate:

(1) Axial symmetry is assumed.

(2) Plasma neutrality is assumed such that $n = n_e \approx n_i$.

(3) The quantity $\partial V/\partial r$ is a function only of r.

(4) U_{zi} is a constant.

(5) n is a function only of z.

(6) U_{ri} is a function only of r.

(7) U_{ze} is a function only of z.

(8) No perturbations arise from influence of the ion beam outside the anode.

Writing out the continuity equations in scalar form with the electron equation of motion (eq. (3)) substituted in them yields

$$\mu_{\perp e} \frac{1}{v} \frac{\partial}{\partial r} \left(r n_e \frac{\partial V}{\partial r} \right) + \frac{\partial}{\partial z} (n_e U_{ze}) = 0 \tag{10}$$

$$\frac{1}{r} \frac{\partial}{\partial r} (r n_i U_{ri}) + \frac{\partial}{\partial z} (n_i U_{zi}) = 0 \tag{11}$$

These partial differential equations can be easily separated using the previous assumptions and the separating constants K' and K'' to yield the following results:

$$U_{ri} = \frac{K' r}{2} \tag{12}$$

$$\frac{\partial V}{\partial r} = \frac{K''r}{2\mu_{\perp e}} + \frac{C_1}{r} \tag{13}$$

$$n = n_0 e^{-(K'/U_{zi})z} \equiv n_0 e^{-Cz} \tag{14}$$

and

$$U_{ze} = \frac{K''}{K'} U_{zi} + C_2 \frac{e^{Cz}}{n_0} \tag{15}$$

The constant C_1 is determined from the boundary condition that the electron current to the metal rod on the axis is zero, because there is no electron emission from the rod, and the plasma electrons are attracted to the anode. Thus, from equation (3), $\partial V/\partial r$ is zero at $r = r_1$, the radius of the rod, so that $C_1 = -K''r_1^2/2\mu_{\perp e}$. Equation (13) then becomes

$$\frac{\partial V}{\partial r} = \frac{K''r}{2\mu_{\perp e}} \left[1 - \left(\frac{r_1}{r} \right)^2 \right] \tag{16}$$

(Sheath effects are neglected in this study because, from table I, the Debye length is small compared with the dimensions of the experiment.) Since the rod radius is small compared with experimental radii, the second term in equation (16) and hence also in equation (13) can be neglected. Integrating equation (13) then yields

$$V = a_1 r^2 + b_1 \tag{17}$$

where a_1 and b_1 are constants.

As a result of the preceding analysis, the behavior of the number density (eq. (14)) and the behavior of the electric potential (eq. (17)) have been deduced. As will be seen in later sections, the exponential in equation (14) was such that, for the experiment, the

behavior of the number density differed only slightly from a linear decline with increasing z.

APPARATUS AND PROCEDURE

Experimental Description

The experimental setup is shown in figure 1. A collimated ion beam supplied from an ion thruster passed through an electrically floating 20-centimeter-long by 5-centimeter-radius cylindrical metal anode with an electrically grounded axially centered metal rod. The anode was electrically connected to a vacuum tube voltmeter of very high input impedance (see sketch (b)), which essentially measured the floating potential of the anode

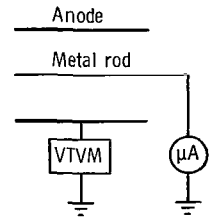

(b)

with respect to ground. Floating potential data were recorded for various magnetic field strengths. A microammeter was used in the metal rod leg to check current flow to this electrode. A small current related to ion impingement was found.

The anode was set inside an axial magnetic field with a field variation of less than 5 percent. Movable molybdenum probes, a description of which is given in the following section, were set at the entrance and exit of the anode and could be moved across the anode diameter. Two movable Langmuir probes were placed inside the anode and were free to move in the anode across a radius. The Langmuir probes were set at the center plane of the anode (z = constant) and were displaced by 120°. The motion of the probes

was obtained through an actuating mechanism driven by a low rpm motor. The probe position was obtained from a potentiometer connected to an ohmmeter calibrated in linear distance.

Typically the ion thruster accelerated to 2000 volts a 50-milliampere beam of mercury ions which were directed along the axis of the experiment. The beam was collimated and limited by a series of baffles before passing through the anode cylinder. About 2 milliamperes of beam current entered the anode, a significant part of which (about 50 percent) impinged on the anode wall. The ion thruster and experimental rig were placed in a vacuum chamber $1\frac{1}{2}$ meters in diameter and 5 meters long which operated at a pressure of 1×10^{-6} to 2×10^{-6} torr (1.3×10^{-4} to 2.6×10^{-4} N/m^2) when the thruster was on. For calculating the classical electron mobility coefficient, it was found convenient, however, to deliberately leak in air raising the pressure to 8×10^{-6} torr (12.4×10^{-4} N/m^2), for with this pressure it can be assumed that the neutral background consists mainly of nitrogen (see table I). Also, with this pressure the plasma potential fell between 10 and 75 volts, a convenient range for biasing the Langmuir probes. Finally a shielding screen was placed slightly beyond the exit of the anode to prevent plasma from contacting the outside surface of the anode cylinder (see fig. 1(a)).

Molybdenum Probe Operation

Sketch (c) shows the molybdenum button probe circuitry. The molybdenum button probe consists of a molybdenum disk about 3 millimeters in diameter facing into the ion beam. The probe is biased negatively by about 20 volts with respect to plasma potential to suppress electron collection. The impinging ion beam current is registered on an X-Y plotter by means of a voltage drop across a 10 000-ohm input resistor and plotted against probe position. The beam current density is obtained by dividing probe current by the area of the disk. The plasma number density can be obtained from equation (1) and the assumption of quasi-neutrality. Values of number density were obtained in this manner at the entrance and exit of the anode, and values of number density in the center plane were obtained by calculations based on equation (14). As was noted previously,

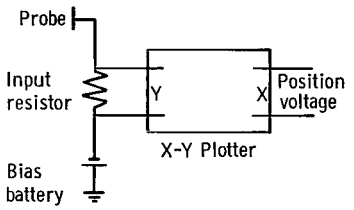

(c)

equation (14) differed only slightly from linear in the present study. In addition to number density data the molybdenum button probes can be used in determining anode ion impingement current, which is equal to electron current for an electrically floating anode. This is simply accomplished by integrating ion current density over the anode entrance area and exit area and then subtracting the ion current leaving the anode from the ion current entering the anode. The Langmuir probes, when operated in the mode shown in sketch (c), can also give number density data by taking into account the probe area subject to ion impingement.

Langmuir Probe Operation

Sketch (d) shows the circuit of the Langmuir probe used in the experiment.

An X-Y plotter was used in conjunction with the Langmuir probe to obtain electron or ion current to the probe as a function of bias potential. A 10 000-ohm input resistor was used. Typical Langmuir probe data for this experiment is indicated in sketch (e). In sketch (e) probe current I_p is plotted against bias potential V_b, and the floating potential V_f is identified as the bias potential corresponding to zero probe current. Typical ranges of I_p and V_b are 0 to 2×10^{-7} ampere and 0 to 50 volts, respectively. In this experiment the Langmuir probe was used to measure radial electric fields. To obtain this quantity, it was necessary to make measurements of plasma potential against radial position. From reference 17 plasma potential can be obtained from floating potential and electron temperature by the following relation,

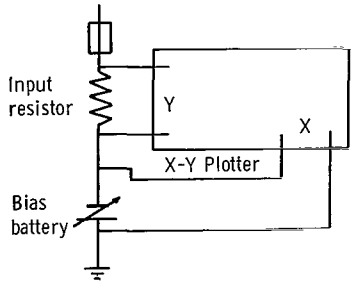

(d)

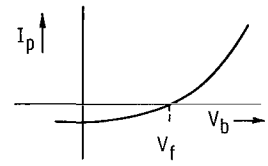

(e)

$$V_{pp} = V_f + g\frac{kT_e}{e} \tag{18}$$

where V_{pp} is plasma potential and $g = 3$ for mercury ions according to reference 17. The electron temperature can be obtained from the slope of a semilog plot of Langmuir probe data using the conventional probe analysis technique. In the experiment, plasma potential was measured at three equally separated radial positions. The inner and outermost potential values were used with equation (17) to obtain the constants a_1 and b_1. The middle potential measurement is used as a simple check of the equation. By differentiation of equation (17), the radial electric field can be obtained.

The aforementioned data (both molybdenum button and Langmuir probe data) were used in equation (2) to determine whether the diffusion process was classical or anomalous. Molybdenum button probe data yielded values of number density and also ion impingement current to the anode (equal to electron flow), while Langmuir probe data yielded measurements of radial electric field. An empirical value of $\mu_{\perp e}$ then was obtained from equation (3) with J_{re}, n, and $\partial V/\partial r$ being taken at the radius of the anode a, and in the center plane of the anode, where $J_{re}(a)$ was assumed to be an average value. This value of $\mu_{\perp e}$ was compared to Bohm's empirical relation (eq. (7)) for different values of magnetic field.

Correlation Technique

According to the theory of anomalous diffusion considered in this report (the Kadomtsev and Nedospasov theory), number density perturbations as well as potential perturbations rotate in the anode cylinder. Both these types of perturbations passing a Langmuir probe will result in an alternating current signal. The signal picked up by the Langmuir probes when the plasma was experiencing anomalous diffusion was found to be a spectrum of many frequencies including a great deal of noise. To pick out the signal corresponding to the rotation (which was believed to be embedded in the noise), a correlation technique was used. Tuned circuits were coupled to two Langmuir probes separated by 120^{o} in the central plane of the anode. Sketch (f) below shows the circuitry in-

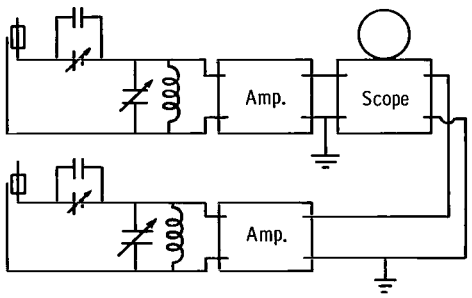

(f)

volved. Both circuits were sharply tuned to the same frequency, the frequency of rotation, and allowed a small frequency band (a band width of about 2 percent of the tuned frequency) consisting of noise and rotation to pass. The signals from the two probes were then applied to a dual beam oscilloscope and one of them triggered both beams. The effect of triggering was to allow many sweeps to fall on top of each other and yield a clear and well-defined trace for the signal controlling the triggering. The shape of the other trace depended on whether or not it had a definite phase relation with the controlling signal. If the second trace contained the rotational signal, then a clear second signal should be obtained on the oscilloscope (since it has a definite phase relation with the controlling signal) with 120° phase shift with respect to the triggering signal. If, however, the signals passing through the tuned circuits were just noise, then the second trace would appear to have a random relation with the first trace. The rotational signals were distinguished from the noise in this manner.

RESULTS AND DISCUSSION

Floating Potential and Plasma Noise

As a result of electrically floating the anode in the exhaust beam of the ion thruster, a positive potential was obtained on the anode with respect to ground. A typical curve of these potentials as a function of magnetic field is shown in figure 2. These values of potential are below 100 volts. With a Langmuir probe placed in the plasma, the anode electrically floating, and a magnetic field applied, noise such as depicted in figure 3 is observed on an oscilloscope connected to the Langmuir probe. This noise, which is deduced to be made up predominantly of a low frequency, is not observed when the anode is grounded (no electron transport) or when the magnetic field strength is less than 20×10^{-4} tesla. These observations and their relation to the diffusion process will be discussed more fully in a later section. First, though, molybdenum probe data and Langmuir probe data will be analyzed and discussed. Anomalous diffusion, which was found to exist in the experiment, will be then discussed in relation to the aforementioned observations.

Molybdenum Probe Data

Current density profiles of the ion beam plasma at the entrance and exit of the anode, obtained with molybdenum button probes, are presented in figures 4 and 5. Also presented in figure 6 is the beam plasma profile at the center plane of the anode obtained with a Langmuir probe operated as a molybdenum button probe. The data presented are for

various values of magnetic field strength and for a floating anode. A most interesting feature of these profiles is their departure from flatness at magnetic fields greater than zero. An explanation for the dip in the center (about $r = 0$) of the back profiles might be that the grounded center rod supporting structure shielded some of the beam from impinging on the molybdenum disk.

The bell shape of the front profiles and the double peaks of the other profiles (observed if the traces are reflected through $r = 0$) which occur with magnetic fields greater than zero is not easy to explain since the ion beam should not be affected by these weak magnetic field strengths. It was further observed, however, that when the anode is electrically grounded the profiles are independent of magnetic field and thus are relatively flat. Note that by itself the radial electric field associated with the floating anode potential should not be strong enough to affect the profile. Since the behavior of the plasma is stable when the anode is electrically grounded and since experimentally the profile is affected by whether or not the anode is floating or grounded, perhaps the changing shapes with magnetic field is linked to the anomalous mode of the plasma; the complete explanation however, has not been deduced.

From entrance and exit molybdenum button probe measurements, values of ion current into and out of the anode are calculated by area integration and are presented in table II. Also presented are values of electron current to the anode (equal to the ion impingement current to the anode), values of C from equation (14), and values of number density at the center plane of the anode. The electron current to the anode is obtained simply by subtracting ion current out from ion current in. Electron number density at the entrance and exit of the anode is obtained (assuming $n_i \approx n_e$) from equation (1) by using the exhaust velocity of the ion thruster and average values of ion current density. Values of number density at the center plane of the anode are obtained by using the aforementioned number densities and equation (14).

For the experimental values of C in the quantity e^{-CZ}, the number density shows an almost linear decline from entrance to exit of the anode. Impingement current to the anode (equal to electron current) and number density at the center of the anode are shown as a function of magnetic field in figure 7.

Langmuir Probe Data

Langmuir probe traces were taken on an X-Y plotter at three equally spaced radial positions in the center plane of the anode for three values of magnetic field strength. The radius of the anode is 5 centimeters and, starting from the center rod, Langmuir probe traces were taken at a 1.25, 2.50, and 3.75 centimeter radii. A typical Langmuir probe trace of current to the probe as a function of bias voltage is shown in figure 8.

This is a replot of a trace from an X-Y plotter in which there was noise variation of $\pm 0.05 \times 10^{-7}$ ampere. From this and similar plots, values of floating potential and Maxwellian temperature were obtained. Figure 9 is a replot of figure 8 on semilog paper. From the slope of this plot, the electron temperature was determined to be 5.1 electron volts. Electron temperatures for the other traces ranged from 3 to 6 electron volts. From values of floating potential and electron temperature, values of plasma potential were obtained using equation (18). Three data points were obtained for each magnetic field strength. These are plotted in figure 10, and curves of the form $a_1 r^2 + b_1$ (see eq. (17)) fit to the end points of each set of three are drawn. The center plasma potential points fall close to the theoretical curves in each case. Resulting values of a_1, b_1, and the calculated values of electric gradient at the anode radius are given in table III. Study of the plasma potential plots of figure 10 and the floating anode potential curve of figure 2 indicates that there is a relatively small voltage drop in the plasma compared to the large sheath drop at the electrically grounded center rod.

Anomalous Diffusion and the Bohm Equation

The classical value of the transverse electron mobility is calculated from equation (5) and plotted as a function of magnetic field in figure 11. The calculation is based on the average value of electron velocity, the average cross section, and a neutral background of nitrogen at the pressure of 8×10^{-6} torr (12.4×10^{-2} N/m^2) mentioned in the section APPARATUS AND PROCEDURE.

Equation (2) is the classical (collisional) equation of electron current flow to the anode in the experiment. Using the number density gradient calculated from figure 6 in the center plane at the anode radius and the classical diffusion coefficient, it is found that the first term in equation (2) is orders of magnitude smaller than the experimentally determined value for $J_{re}(a)$. For this reason, its contribution can be neglected. Equation (3) was then used to determine whether the experimental diffusion process was classical. Substituting into equation (3) average values of electron current density, center plane values of number density, and experimental values of electric field gradient yielded computed values for the electron mobility. Comparison of these values with the theoretical values plotted in figure 11 showed that experimental values were much higher. For example, for a magnetic field of 55×10^{-4} tesla the calculated value of the mobility was 20 square meters per volt per second whereas from figure 11 the theoretical value is 5×10^{-3} square meters per volt per second. Similar differences in the electron mobility coefficient existed for the other magnetic field values investigated. These results are orders of magnitude different and strongly suggest that anomalous diffusion is occurring in the range of magnetic fields in the experimental study. Further evidence of anomalous

diffusion can be obtained if equation (3) is solved for electric field using theoretical values of collisional mobility and experimental values of number density and current density. Resulting values of electric field are in the range of 10^4 and 10^5 volts per meter, which would indicate a floating anode potential of thousands of volts across the 5-centimeter gap. This is inconsistent with the floating anode potentials of figure 2.

As previously stated, plasma noise was detected with a floating Langmuir probe when the anode was electrically floated and a magnetic field was applied. The frequency of the noise was determined to range from 0 to 200 kilohertz per second. The noise was unobservable with the same instrumentation setup when the anode was electrically grounded or when the magnetic field dropped below about 20×10^{-4} tesla. It has been noted in many studies (see, for example, ref. 10) that low frequency plasma noise occurs in conjunction with anomalous diffusion and further that the onset of anomalous diffusion was also the onset of low frequency noise in the same frequency range observed here. This would indicate (1) that the onset of anomalous diffusion is about 20×10^{-4} tesla in this study and (2) that anomalous diffusion did not exist for an electrically grounded anode. Both conclusions are consistent with the Kadomtsev and Nedospasov theory.

First anomalous diffusion occurred above 20×10^{-4} tesla which means transition to anomalous diffusion in the experiment occurs in the "tens of gauss" range. In reference 4, the pressure involved was about 1 torr (1.3×10^2 N/m^2), and the critical magnetic field occurred in the "thousands of gauss" range; in reference 6, the pressure was 10^{-3} torr (1.3×10^{-1} N/m^2) and the onset occurred in the "hundreds of gauss" range. In the present experiment, the pressure is about 10^{-6} torr (1.3×10^{-4} N/m^2) (see table I), and the onset occurring in the "tens of gauss" range is consistent with the general concept of lower critical fields with lower pressure. Finally, grounding the anode probably destroys the radial electric field (see eq. (18) with $K = 0$) and anomalous diffusion, which depends on electrons drifting in this electric field, therefore does not exist.

Empirical values of electron mobility for three different values of magnetic field were obtained as before from equation (3) by substituting into it experimentally determined values of electron current density, number density, and electric field gradient. These values are plotted in figure 12. The object is to see if Bohm's diffusion equation (eq. (7)) is applicable. A plot of C_B/B is drawn in figure 12 for C_B taken as 0.12 (which was found to be a good fit to the data). It can be concluded that the mobility behaves as B^{-1} (but with a coefficient C_B two times greater than Bohm's value). In this respect Bohm's equation is applicable to the data obtained herein. In reference 15 it was also found that the coefficient C_B was about 2 times greater than Bohm's value, although other values have been found by other investigators (e.g., ref. 14).

Rotational Study

Rotation of a number density concentration and potential gradient perturbation is intrinsic to the Kadomtsev and Nedospasov approach to instability in a plasma with a neutral background. Both conditions can induce an alternating current signal on a Langmuir probe placed in the plasma. A correlation technique described in a preceding section was used to detect rotation in the beam plasma. The plasma in the device studied in reference 7 was found to rotate with a velocity equal to one-fifth the velocity determined by the radial electric field $\left[(1/5)(E_r/B)\right]$. The plasma in the device studied in reference 18 rotated with a velocity equal to that determined by the radial electric field E_r/B when the magnetic field was greater than the critical field. The rotational frequency for a rotational velocity of E_r/B is

$$f = \frac{1}{2\pi r}\left[\frac{E_r(r)}{B}\right] \tag{19}$$

for the $m = 1$ mode usually considered. From equation (17) this frequency is independent of r.

The correlation technique was used to determine whether rotation could be found in the frequency range of equation (19) (i.e., 105 to 150 kHz/sec for the magnetic and electric field range in the experiment). First, however, the tuned circuits were set at 88 kilohertz per second, outside the rotational frequency range of the experiment, and the magnetic field was varied. A typical result is shown in figure 13. The lower signal in this figure as well as in all subsequent figures is the triggering signal. The lack of a clear upper trace in figure 13 indicates no significant correlation. The frequency was then adjusted to 125 kilohertz per second. Figure 14 resulted when the magnetic field was set at 45×10^{-4} tesla. Correlation is apparent with the larger signal on top out of phase with the lower signal by about 125°. This is quite close to the 120° phase difference in the Langmuir probe positions. The lower amplitude signal visible on top appears to be the result of another mode in the plasma rotation. Next, the tuned circuits are set at 140 kilohertz per second and correlation is found at a magnetic field of 97×10^{-4} tesla as shown in figure 15. The phase shift here is about 136°. Finally with the same settings the magnetic field leads are reversed and figure 16 resulted (a slight amount of returning was necessary). In this figure the upper wave is shifted forward, by about 117°, instead of backward as in the previous figure, in just the manner expected for rotation under the influence of a reversed magnetic field.

A plot of equation (19) is shown in figure 17 with frequency of rotation as a function of magnetic field represented. Values of electric field required in equation (19) were

taken from table III. Plotted also, as two experimental points, are the correlation data from figures 14 and 15. The points lie close to the curve consistent with equation (19) as the proper rotational frequency.

Anomalous Diffusion with Respect to the Ion Thruster

In reference 3 a calculation of the Kadomtsev and Nedospasov type was made to determine the boundary between stability and instability of the ionization chamber of an ion thruster. There was indication of anomalous diffusion in the ion thruster beyond a critical magnetic field in the form of noise measurements in the discharge chamber as well as in discharge chamber efficiency (ion loss per beam ion as a function of magnetic field). In the present experiment more direct plasma measurements were made from which anomalous diffusion was deduced. It is interesting to compare the two situations. Both cases deal with partially ionized plasmas. Both have cylindrical configurations with longitudinal magnetic fields, and both have associated radial electric fields in the plasmas. Rotation has been found in the present experiment but has not yet been definitely found in the ion thruster chamber. Both cases show an onset of low frequency noise and are anomalous in the noisy region (ref. 3).

The similarities between the present experiment and the ion thruster discharge chamber suggest that the anomalous diffusion predicted in the ion thruster may result from the same type of mechanism as that obtained in this experiment. If true, this suggests that stabilizing magnetic field configurations (ref. 19) should be investigated as a possible means of reducing these loss mechanisms in the ion thruster discharge chamber.

CONCLUDING REMARKS

An electrically floating anode was set in a neutralized ion beam accelerated from an ion thruster. A theoretical study was made to determine whether the transport characteristics were of the classical or anomalous mode for the configuration. Floating anode potential data, molybdenum button and Langmuir probe data as well as correlation data were taken. Furthermore, low frequency noise from a Langmuir probe was observed for various magnetic fields and for a floating anode condition. As a result of this study, anomalous diffusion was found, and its onset occurred at a low magnetic field strength. A relation between anomalous diffusion of the Kadomtsev and Nedospasov type and Bohm diffusion equation was thought to be linked by the Hall effect. Bohms equation was found to agree with experiment if the Bohm coefficient was increased by a factor of 2. Since the Kadomtsev and Nedospasov approach appeared applicable, a correlation study was

undertaken in order to find rotation. Rotation was found at the predicted values ranging from 100 to 150 kilohertz per second. The report supports many previous studies in predicting the onset of anomalous diffusion in a plasma with crossed magnetic and electric fields.

It was speculated that the electron diffusion in an ion thruster discharge may be the same type as that observed herein. If so, the loss might be alleviated with a stabilizing magnetic field configuration.

Lewis Research Center,
National Aeronautics and Space Administration,
Cleveland, Ohio, May 20, 1968,
120-26-02-10-22.

APPENDIX - SYMBOLS

a	anode radius
a_1, b_1	constants in eq. (17)
B	magnetic field strength
C	K'/U_{zi}
C_B	Bohm's constant
C_D	constant
C_1, C_2	constants
$D_{\perp e}$	electron transverse diffusion coefficient
E	electric field
e	electron charge
I	current
J	current density
J_B	beam current density
K', K''	separation constants
l	length
m_e	electron mass
N_o	neutral number density
n	plasma number density
n_0	$n(z = 0)$
r	r-coordinate
r_1	radius of centered rod
T_e	electron temperature
U	drift velocity
U_{zi}	ion beam velocity
V	electric potential
v	velocity
x	x-coordinate on oscilloscope
y	y-coordinate on oscilloscope
z	z-coordinate
θ	θ-coordinate
λ_e	Debye distance
$\mu_{\perp e}$	electron transverse mobility
σ	cross section
τ_e	electron collision time
ω_e	electron cyclotron frequency

Subscripts:

b	bias
e	electron
f	floating
i	ion
p	probe
pp	plasma
r	r-coordinate
t	total
z	z-coordinate
θ	θ-coordinate

REFERENCES

1. Kaufman, Harold R.: An Ion Rocket With An Electron-Bombardment Ion Source. NASA TN D-585, 1961.

2. Mickelsen, William R.; and Kaufman, Harold R.: Status of Electrostatic Thrusters for Space Propulsion. NASA TN D-2172, 1963, p. 16.

3. Cohen, Allan J.: Onset of Anomalous Diffusion in Electron-Bombardment Ion Thruster. NASA TN D-3731, 1966.

4. Kadomtsev, B. B.; and Nedospasov, A. V.: Instability of the Positive Column in a Magnetic Field and the "Anomalous" Diffusion Effect. J. Nucl. Energy, Part C, Plasma Phys., vol. 1, 1960, pp. 230-235.

5. Guest, Gareth; and Simon, Albert: Instability In Low-Pressure Plasma Diffusion Experiments. Phys. Fluids, vol. 5, no. 5, May 1962, pp. 503-509.

6. Hoh, F. C.: Instability of Penning-Type Discharges. Phys. Fluids, vol. 6, no. 8, Aug. 1963, pp. 1184-1191.

7. Janes, G. S.; and Lowder, R. S.: Anomalous Electron Diffusion and Ion Acceleration in a Low-Density Plasma. Phys. Fluids, vol. 9, no. 6, June 1966, pp. 1115-1123.

8. Boeschoten, F.: Review of Experiments On the Diffusion of Plasma Across a Magnetic Field. J. Nucl. Energy, Part C, Plasma Phys., vol. 6, no. 4, July/Aug. 1964, pp. 339-388.

9. Chapman, Sydney; and Cowling, T. G.: The Mathematical Theory of Non-Uniform Gases. Cambridge University Press, 1939.

10. Guthrie, A.; and Wakerling, R. K., eds.: The Characteristics of Electrical Discharges in Magnetic Fields. McGraw-Hill Book Co., Inc., 1949.

11. Spitzer, Lyman, Jr.: Particle Diffusion Across a Magnetic Field. Phys. Fluids, vol. 3, no. 4, July-Aug. 1960, pp. 659-661.

12. Drummond, William E.; and Rosenbluth, Marshall N.: Anomalous Diffusion Arising from Microinstabilities in a Plasma. Phys. Fluids, vol. 5, no. 12, Dec. 1962, pp. 1507-1513.

13. Yoshikawa, S.; and Rose, D. J.: Anomalous Diffusion of a Plasma Across a Magnetic Field. Phys. Fluids, vol. 5, no. 3, Mar. 1962, pp. 334-340.

14. Schwirzke, Fred: Reduced Plasma Diffusion in Positive Gradient Magnetic Field Configurations. Phys. Fluids, vol. 10, no. 1, Jan. 1967, pp. 183-188.

15. Geissler, K. H.: Investigation of the Diffusive Decay of a Plasma Contained in a Conducting Cylinder in the Presence of a Magnetic Field. Rep. IPP-2/51, Institut Für Plasmaphysik, West Germany, Sept. 1966.

16. Dodo, T.: Anomalous Diffusion of an Afterglow-Plasma. Rep. IPP-2/62, Institut Für Plasmaphysik, West Germany, May 1967.

17. Schwirzke, Fred: Electric Fields Caused by the Diffusion of Charged Particles Across a Magnetic Field. Phys. Fluids, vol. 9, no. 11, Nov. 1966, pp. 2244-2249.

18. Chen, Francis F.; and Cooper, Alfred W.: Electrostatic Turbulence in a Reflex Discharge. Phys. Rev. Letters, vol. 9, no. 8, Oct. 15, 1962, pp. 333-335.

19. Thomassen, K. I.: Turbulent Diffusion in a Penning-Type Discharge. Phys. Fluids, vol. 9, no. 9, Sept. 1966, pp. 1836-1842.

TABLE I. - CONSTANTS IN THE EXPERIMENT

Neutral number density, N_o, m^{-3}	2×10^{17}
Average cross section, $\bar{\sigma}$, m^2	14×10^{-18}
Electron collision time, τ_e, sec	36×10^{-6}
Electron temperature, kT_e/e, eV	3 to 6
Debye distance, λ_e, m	0.5×10^{-2}
$\omega_e\tau_e$ (B = 10×10^{-4} tesla)	6500
$\omega_e\tau_e$ (B = 100×10^{-4} tesla)	65 000

TABLE II. - COMPUTED RESULTS BASED ON MOLYBDENUM DATA

Magnetic field, B, tesla	Ion beam current, mA		Electron current to anode, mA	C, [a] 1/m	Number density, n, m^{-3}
	In	Out			
0×10^{-4}	1.54	0.77	0.77	2.76	1.88×10^{13}
[b]28	----	----	[b].92	----	[b]2.15
55	1.99	.90	1.09	3.16	2.34
108	2.30	.81	1.5	4.16	2.46

[a]Coefficient in eq. (14).

[b]Extrapolated value.

TABLE III. - COMPUTED RESULTS BASED ON LANGMUIR PROBE DATA

Magnetic field, B, tesla	a_1, [a] V/m^2	b_1, [a] V	Electric field at r = a, V/m
28×10^{-4}	960	33.95	96
55	2240	42.3	224
108	5120	43.1	512

[a]Coefficient in eq. (17).

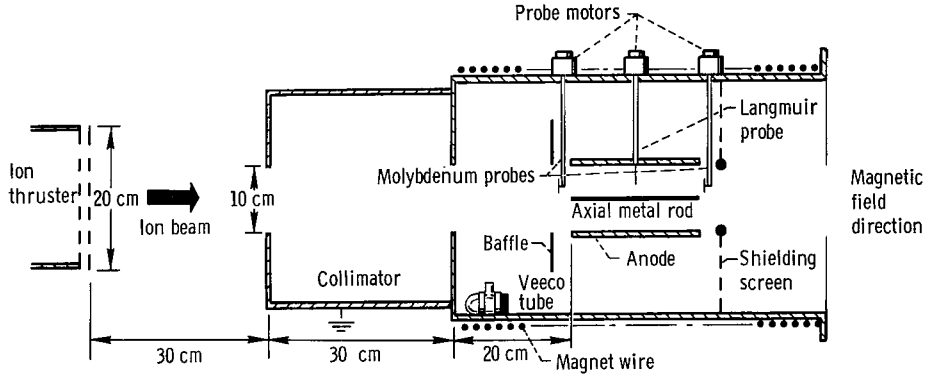

(a) Schematic.

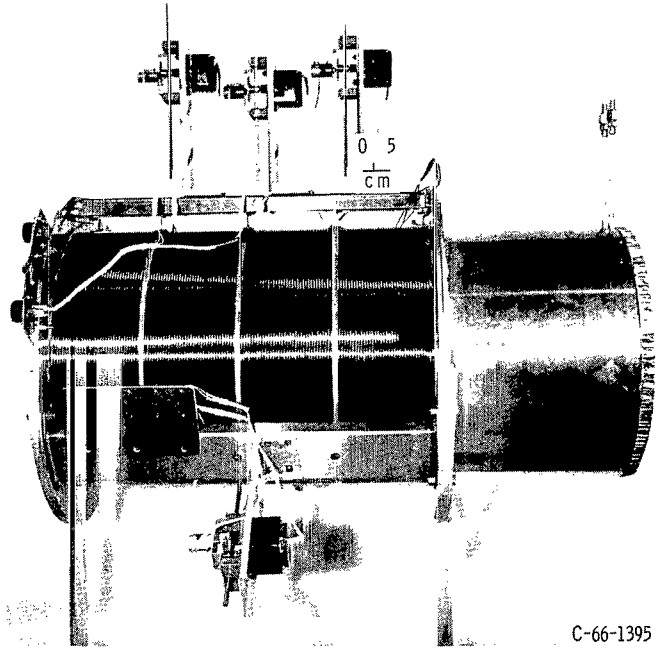

(b) Exterior view.

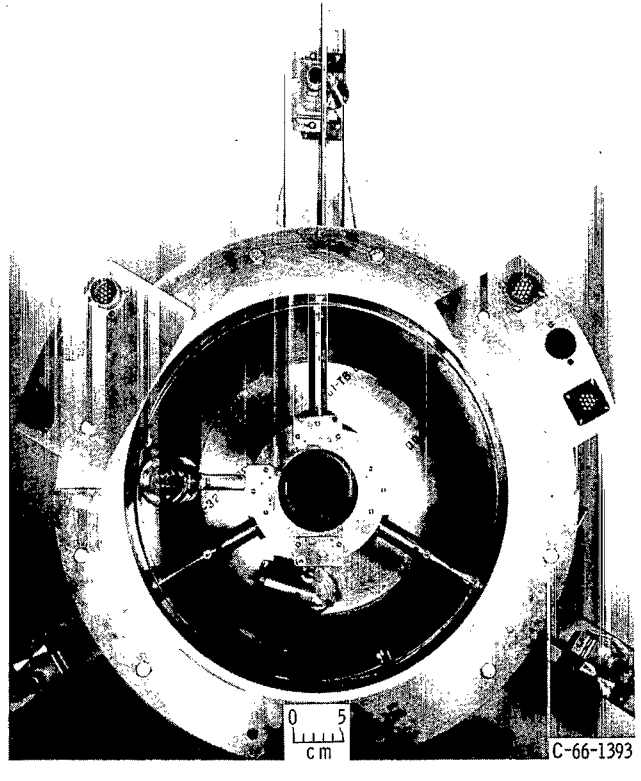

(c) Internal view.

Figure 1. - Experimental configuration.

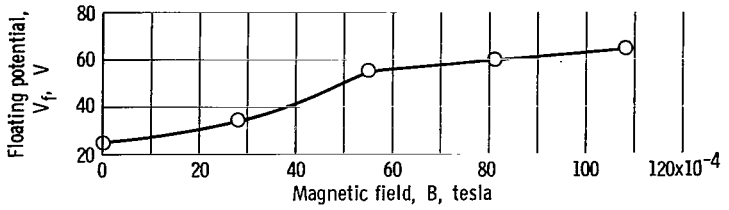

Figure 2. - Floating potential as a function of magnetic field.

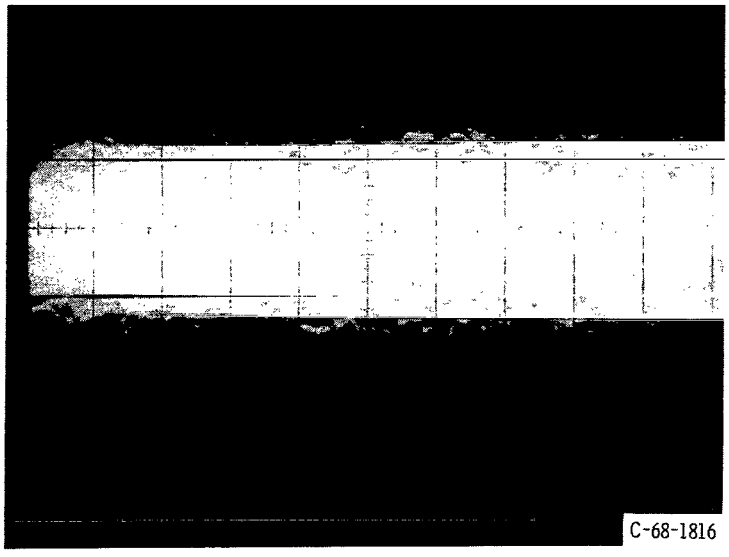

Figure 3. - Plasma noise for magnetic field value of 50x10^{-4} tesla and a floating anode; x = 2 microseconds per centimeter, y = 10 millivolts per centimeter.

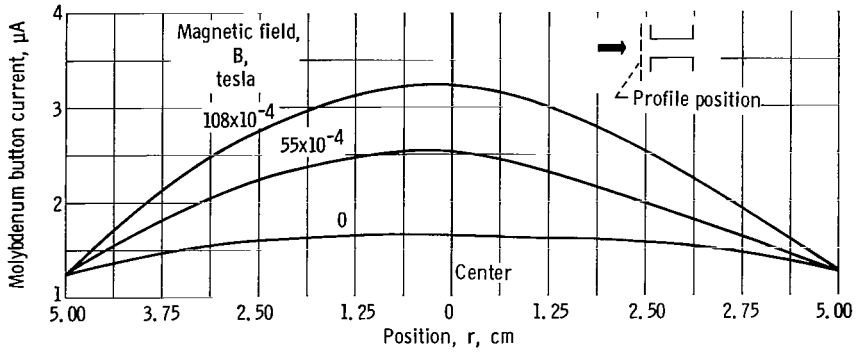

Figure 4. - Molybdenum button front profile for various values of magnetic field. Retrace from X-Y plotter.

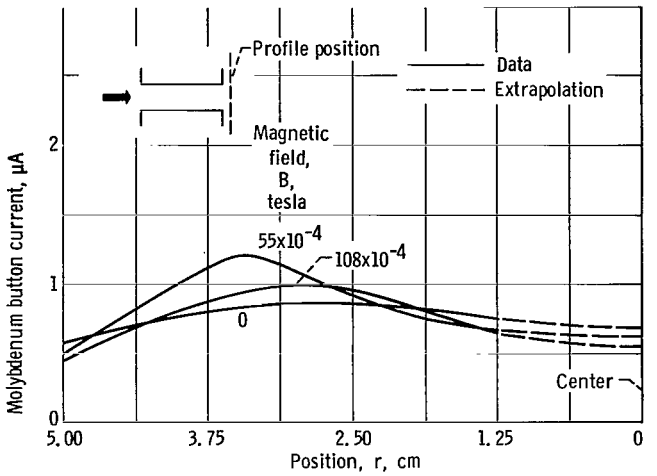

Figure 5. - Molybdenum button back profile for various values of magnetic field. Retrace from X-Y plotter.

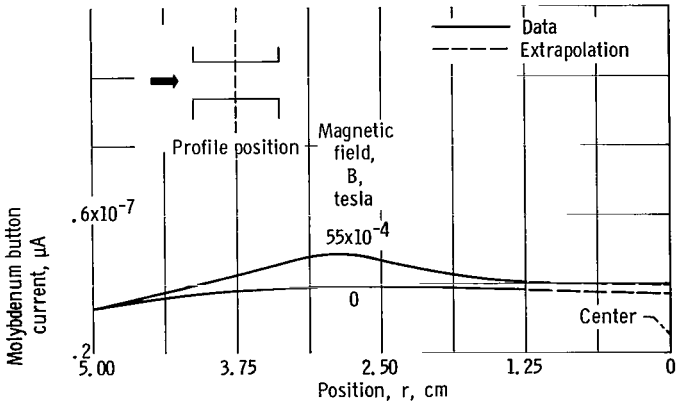

Figure 6. - Molybdenum button data from Langmuir probe for various values of magnetic field. Retrace from X-Y plotter.

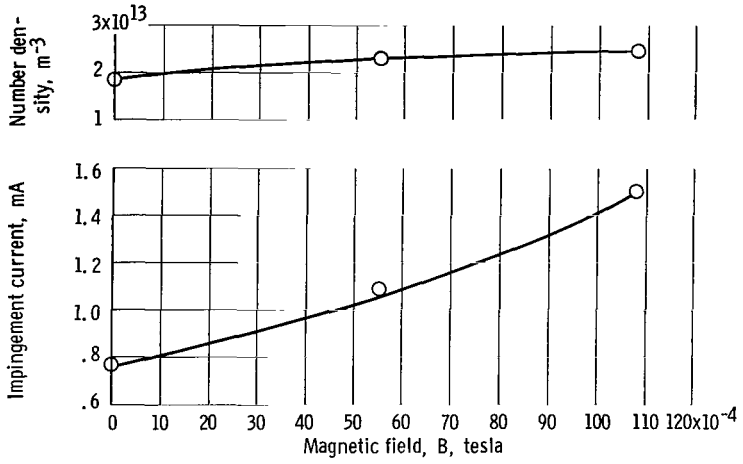

Figure 7. - Anode impingement current and center plane number density as a function of magnetic field.

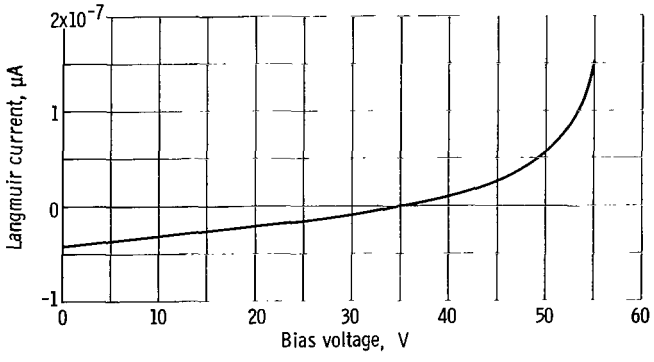

Figure 8. - Langmuir probe trace. Magnetic field, $108x10^{-4}$ tesla; radial position, 3.75 centimeters. Retrace from X-Y plotter.

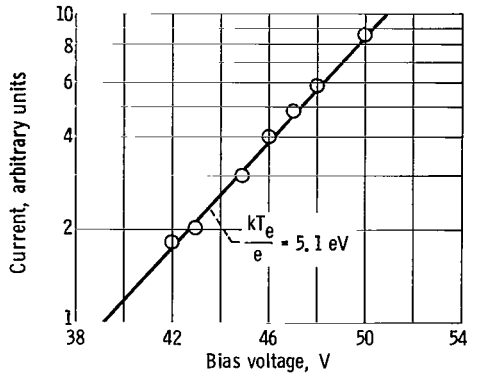

Figure 9. - Log plot of Langmuir probe data from figure 8. Magnetic field, 108×10^{-4} tesla; radial position, 3.75 centimeters.

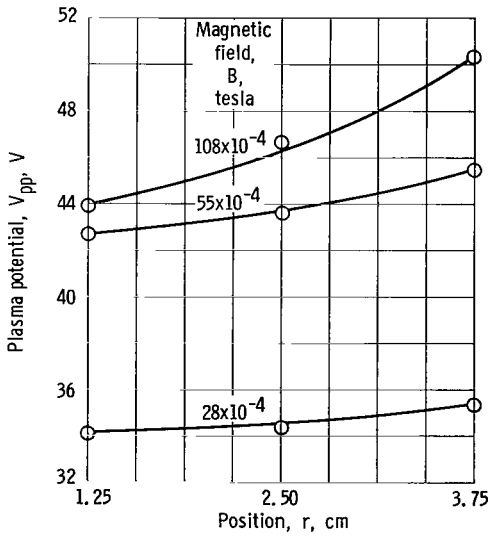

Figure 10. - Plasma potential as a function of radial position for various magnetic fields.

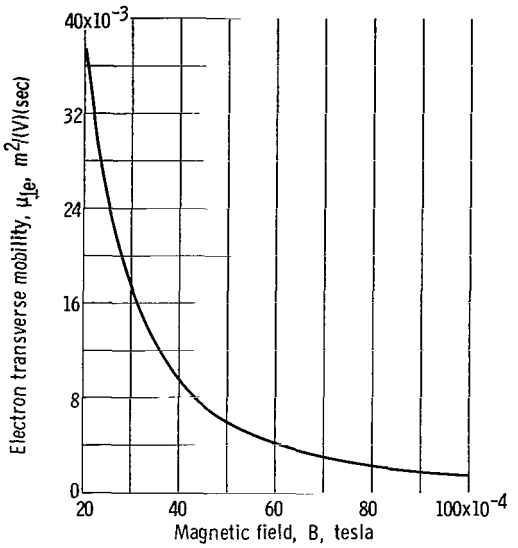

Figure 11. - Calculated classical electron mobility as a function of magnetic field (eq. (5)) for constants appropriate to present experiment. Neutral number density, 2×10^{17} meter^{-3}; average cross section, 14×10^{-18} square meters; average velocity, 10^6 meters per second.

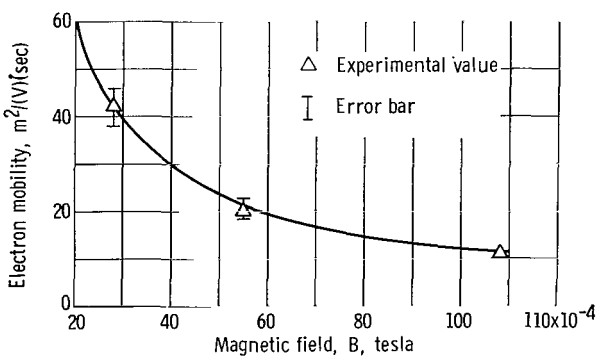

Figure 12. - Comparison of experimental values to theoretical Bohm's equation (with Bohm's constant $C_B = 0.12$ (m^2)(T)/(V)(sec)).

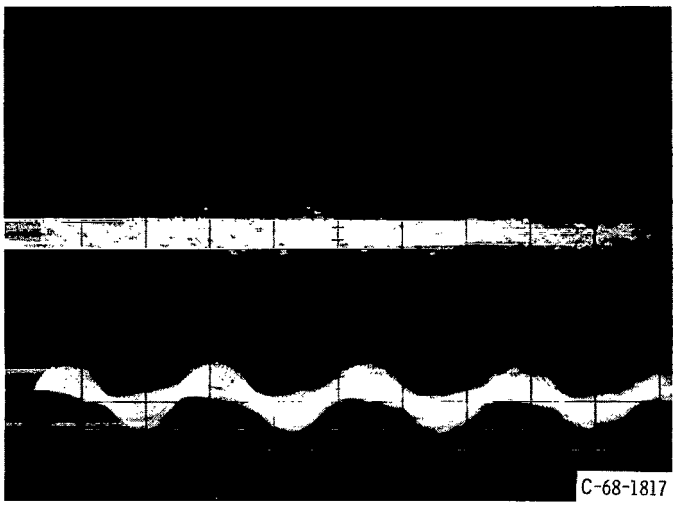

Figure 13. - Correlation study for 88 kilohertz per second. Magnetic field, 55×10^{-4} tesla; x = 5 microseconds per centimeter, y = 10 millivolts per centimeter; probe phase shift, 120°.

Figure 14. - Correlation study for 125 kilohertz per second. Magnetic field, 45×10^{-4} tesla; x = 2 microseconds per centimeter, y = 10 millivolts per centimeter; phase shift, 125°.

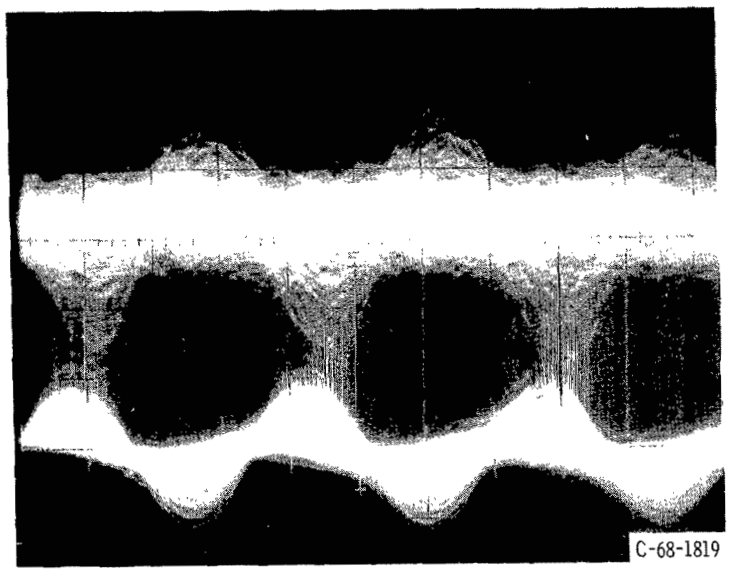

Figure 15. - Correlation study for 140 kilohertz per second. Magnetic field, 97×10^{-4} tesla; x = 2 microseconds per centimeter; y = 10 millivolts per centimeter; phase shift, 136°.

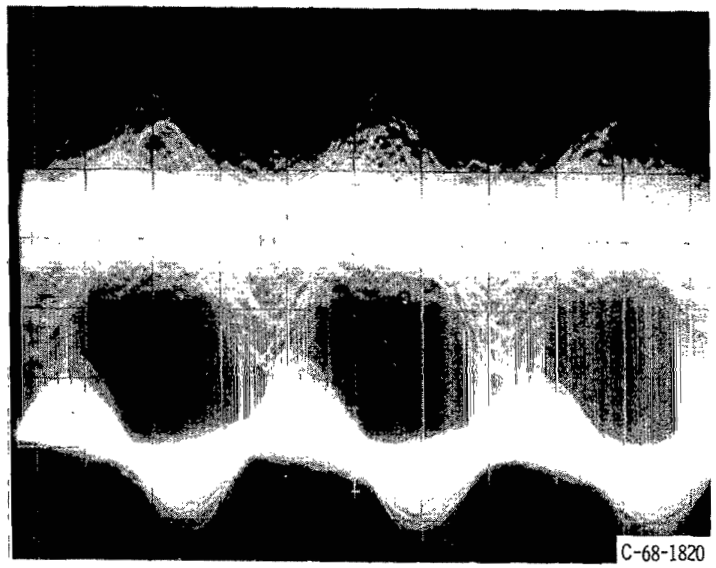

Figure 16. - Correlation study for 140 kilohertz per second. Magnetic field, 97×10^{-4} tesla with magnetic field reversed; x = 2 microseconds per centimeter; y = 10 millivolts per centimeter; phase shift, 117°.

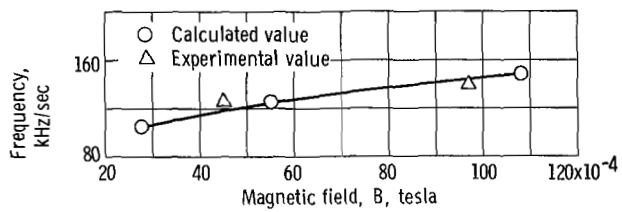

Figure 17. - Rotational frequency as a function of magnetic field strength.

NATIONAL AERONAUTICS AND SPACE ADMINISTRATION
WASHINGTON, D. C. 20546
OFFICIAL BUSINESS

FIRST CLASS MAIL

POSTAGE AND FEES PAID
NATIONAL AERONAUTICS AND
SPACE ADMINISTRATION

"The aeronautical and space activities of the United States shall be conducted so as to contribute . . . to the expansion of human knowledge of phenomena in the atmosphere and space. The Administration shall provide for the widest practicable and appropriate dissemination of information concerning its activities and the results thereof."

—NATIONAL AERONAUTICS AND SPACE ACT OF 1958

NASA SCIENTIFIC AND TECHNICAL PUBLICATIONS

TECHNICAL REPORTS: Scientific and technical information considered important, complete, and a lasting contribution to existing knowledge.

TECHNICAL NOTES: Information less broad in scope but nevertheless of importance as a contribution to existing knowledge.

TECHNICAL MEMORANDUMS: Information receiving limited distribution because of preliminary data, security classification, or other reasons.

CONTRACTOR REPORTS: Scientific and technical information generated under a NASA contract or grant and considered an important contribution to existing knowledge.

TECHNICAL TRANSLATIONS: Information published in a foreign language considered to merit NASA distribution in English.

SPECIAL PUBLICATIONS: Information derived from or of value to NASA activities. Publications include conference proceedings, monographs, data compilations, handbooks, sourcebooks, and special bibliographies.

TECHNOLOGY UTILIZATION PUBLICATIONS: Information on technology used by NASA that may be of particular interest in commercial and other non-aerospace applications. Publications include Tech Briefs, Technology Utilization Reports and Notes, and Technology Surveys.

Details on the availability of these publications may be obtained from:

SCIENTIFIC AND TECHNICAL INFORMATION DIVISION

NATIONAL AERONAUTICS AND SPACE ADMINISTRATION

Washington, D.C. 20546